Supporting information for

Persistent room temperature phosphorescence films based on star-shaped organic emitters

Haiyang Shu,[ab] Liang Chen,[ab] Xiaofu Wu,[a] Tong Wang,[ab] Shuai Wang,[ab] Hui Tong*[ab] and Lixiang Wang*[ab]

[a] State Key Laboratory of Polymer Physics and Chemistry, Changchun Institute of Applied Chemistry, Chinese Academy of Sciences, Changchun 130022, China
[b] School of Applied Chemistry and Engineering, University of Science and Technology of China, Hefei 230026, China

Corresponding Author
* E-mail: chemtonghui@ciac.ac.cn; lixiang@ciac.ac.cn

Table of contents

Page

1. Experimental details

General information: ^{1}H-NMR, ^{19}F-NMR and ^{13}C-NMR spectra were measured using Bruker Avance NMR spectrometer at 25^{o}C unless noted. Gas chromatography-mass spectrometry (GC-MS) was measured with agent 5975. Matrix-assisted laser desorption/ ionization time of flight (MALDI-TOF) mass spectra were measured on AXIMA CFR MS apparatus (COMPACT).

Photophyiscal measurements: UV/Vis absorption spectra were measured by a Perkin–Elmer Lambda 35 UV/Vis spectrometer. Photoluminescence (PL) measurements were conducted utilizing FluoroMax-4 spectrophotometer equipped with a 150 W xenon lamp as the excitation source. The quantum yields were measured on an integrating sphere (Hamamatsu Photonics C9920-2). Fluorescence lifetimes and phosphorescence lifetimes were measured with an Edinburgh FLSP-980 fluorescence spectrophotometer. Fluorescence lifetime is using picoseconds pulsed lasers (EPLSs) as the excitation source and time correlated single photon counting (TCSPC) as data acquisition technique. Phosphorescence lifetime is using a 60 W xenon flashlamp (μF2) as the excitation source and multi-channel scaling (MCS) for time resolved photon counting as data acquisition technique. X-ray diffraction (XRD) patterns were obtained by using a Bruker D8 Discover thin-flm diffractometer. Atomic force microscopy (AFM) images were measured with the SPI3800 N Probe Station and SPA-300HV unit system (Seiko Instruments Inc., Japan) in tapping mode.

Device fabrication and characterization: The glass substrates coated with indium tin oxide (ITO) (15 Ω per square) were washed with acetone, isopropanol and deionized water successively, and were dried under 120^{o}C for 45 min. Then the substrates were treated by ultraviolet–ozone for 45 min. Subsequently PEDOT:PSS (Clevious P AI4083) was spin-coated on the substrates to form a film and annealed at 120^{o}C for 1 h. After transferring the substrates into glovebox filled with N_2, solutions of the CzS and Bis[2-(diphenylphosphino)phenyl] ether oxide (DPEPO) in chlorobenzene were spin-coated on PEDOT:PSS layer to form the emissive layer. The substrates were then moved into a vacuum chamber where TSPO1 and TmPyPB were evaporated successively on top of the emissive layer at a pressure less than 4×10^{-4} Pa. Finally, LiF (1 nm) and Al (100 nm) were deposited as the cathode. The J–V–L characteristics of the OLEDs were measured under ambient atmosphere using Keithley 2400/2000 source meter equipped with a calibrated silicon photodiode. EL spectra were measured by a PR650 spectra colorimeter. EQE of the devices were calculated based on the J–L characteristics and the corresponding EL spectra assuming a Lambertian emission distribution.

Synthesis: All the materials used for the synthesis were purchased from commercial sources without further purification unless noted. The carbazole is synthesized in the laboratory according to the literature.[1] Solvents for chemical synthesis were purified according to the standard procedures.

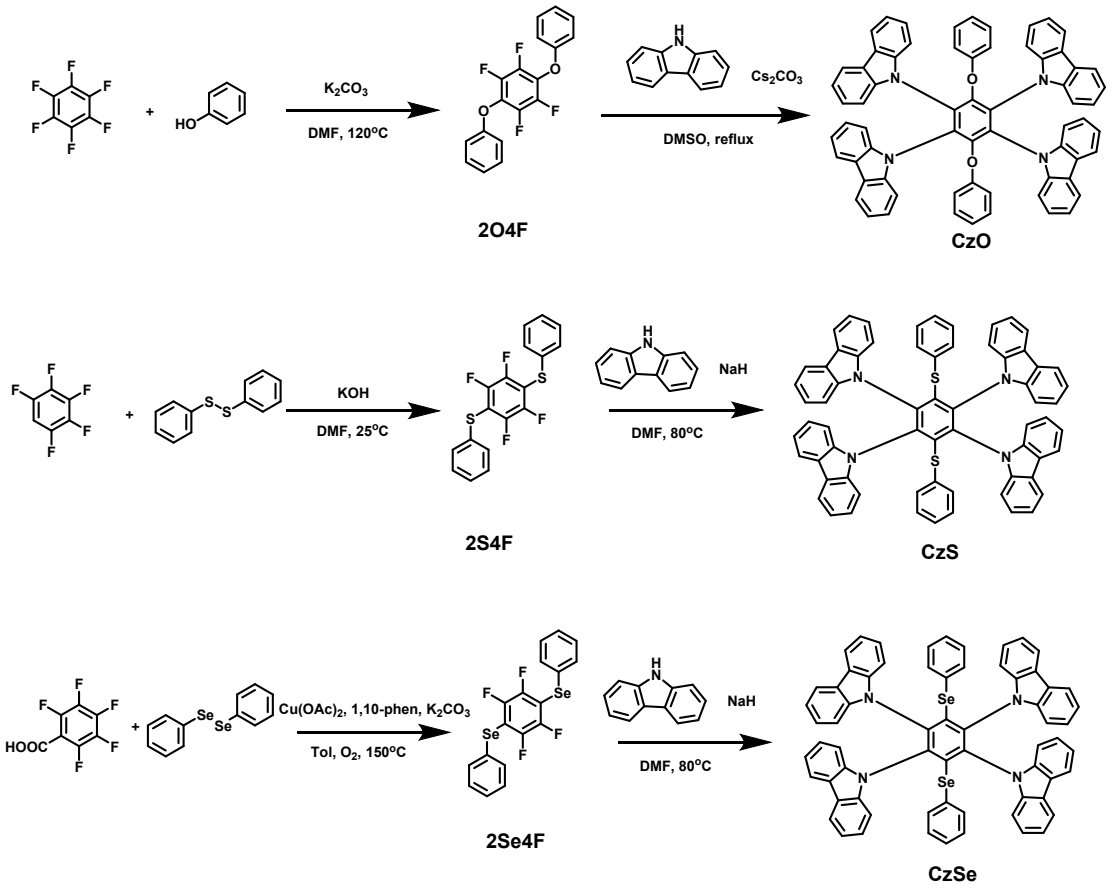

Scheme S1. Synthetic routes of the target compounds.

2,3,5,6-Tetrafluor-1,4-diphenoxy-benzol(2O4F)

Hexafluorobenzene (10.0 mmol, 1.86 g) was added to a solution of phenol (20.0 mmol, 1.88 g) and potassium carbonate (22.0 mmol, 3.04 g) in N,N-dimethylformamide (DMF) under argon. The reaction system was reacted at 150°C for 2 h. After cooling to room temperature, deionized water was added and stirred for 30 minutes. The mixture was filtered and the filter cake was collected. The crude product was purified by silica gel column chromatography (petroleum ether) to afford the product as a white solid (2.0 g, 60%). ^{1}H NMR (500 MHz, $CDCl_3$) δ 7.40 – 7.32 (m, 2H), 7.18 – 7.11 (m, 1H), 7.00 (d, J = 8.0 Hz, 2H); ^{19}F NMR (471 MHz, $CDCl_3$) δ -154.31 (s, 1H); ^{13}C NMR (101 MHz, $CDCl_3$) δ 157.24, 129.88, 123.83, 123.70, 115.50, 115.34. GC-MS (m/z) calcd for $C_{18}H_{10}F_4O_2$ $[M]^+$: 334; Found: 334.

9,9',9'',9'''-(3,6-diphenoxybenzene-1,2,4,5-tetrayl)tetrakis(9H-carbazole)(CzO)

Anhydrous dimethyl sulfoxide (DMSO) was added to a two-neck bottle containing 2O4F (3 mmol, 1.20 g), carbazole (18 mmol, 3.00 g) and cesium carbonate (72 mmol, 23.47 g) under argon. The reaction system was reacted at 230°C for 3 h. After cooling to room temperature, deionized water was added and stirred for 30 minutes. The mixture was filtered and the filter cake was collected. The crude product was purified by silica gel column chromatography (petroleum ether

/dichloromethane=1/2, v/v) to afford the product, followed by recrystallization from tetrahydrofuran (THF) to afford CzO (2.49 g, 75%) as a white solid. ^{1}H NMR (500 MHz, DMSO) δ 8.05 (d, J = 8.1 Hz, 8H), 7.64 (d, J = 7.5 Hz, 8H), 7.19 (t, J = 7.6 Hz, 8H), 6.96 (t, J = 7.3 Hz, 8H), 6.30 (t, J = 7.6 Hz, 4H), 6.12 (t, J = 7.2 Hz, 2H), 6.07 (d, J = 8.0 Hz, 4H). MALDI TOF-MS: calcd for $C_{66}H_{42}N_4O_2[M]^+$: 922.3; found: 922.3.

(perfluoro-1,4-phenylene)bis(phenylsulfane)(2S4F)[2]

Pentafluorobenzene (40 mmol, 6.72 g) was added to a solution of diphenyl disulfide (80 mmol, 17.44 g) and potassium hydroxide (80 mmol, 4.48 g) in N,N-dimethylformamide (DMF) under argon. The mixture was stirred overnight at 25°C. After the reaction was completed, deionized water was added and stirred for 10 minutes. After three times extractions with ethyl acetate, the oil phase was collected, washed three times with a saturated aqueous sodium chloride (NaCl) solution, and the solvent was removed under vacuum. The crude product was purified by silica gel column chromatography (petroleum ether) to afford the product as a white solid (18.13 g, 90%). ^{1}H NMR (500 MHz, $CDCl_3$) δ 7.38 (td, *J* = 8.0, 3.4 Hz, 4H), 7.33 – 7.27 (m, 6H). ^{19}F NMR (471 MHz, $CDCl_3$) δ -132.03 (s, 1H). ^{13}C NMR (101 MHz, $CDCl_3$) δ 132.58, 130.99, 129.41, 128.10. GC-MS (m/z) calcd for $C_{18}H_{10}F_4S_2$ $[M]^+$: 366; Found: 366.

9,9',9'',9'''-(3,6-bis(phenylthio)benzene-1,2,4,5-tetrayl) tetrakis(9H-carbazole) (CzS)

60% NaH (144 mmol, 5.76 g) was added to carbazole (18 mmol, 3.00 g) in 100 mL DMF. After reacting at room temperature for 30 minutes, a DMF (100 mL) solution of 2S4F (3 mmol, 1.10 g) was added to the system and reacted for 15 h at 80°C. After cooling to room temperature, deionized water was added and stirred for 30 minutes. The mixture was filtered and the filter cake was collected. The crude product was purified by silica gel column chromatography (petroleum ether /dichloromethane=1/2, v/v) to afford the product, followed by recrystallization from THF to afford CzS (2.0 g, 70%) as a white solid. ^{1}H NMR (500 MHz, $CDCl_3$) δ 7.62 (d, *J* = 7.6 Hz, 8H), 7.16 (d, *J* = 8.1 Hz, 8H), 7.11 – 7.06 (m, 8H), 7.00 – 6.97 (m, *J* = 7.0 Hz, 8H), 6.33 –6.25 (m, *J* = 21.4, 7.1 Hz, 6H), 6.19 – 6.09 (m, 4H). ^{13}C NMR (101 MHz, DMSO, 110℃) δ 140.54, 139.88, 131.77, 130.41, 128.23, 127.13, 124.95, 123.30, 120.11, 119.71, 112.11. MALDI TOF-MS: calcd for $C_{66}H_{42}N_4S_2[M]^+$: 954.3; found: 954.3.

(perfluoro-1,4-phenylene) bis(phenylselane)(2Se4F)[3]

Anhydrous toluene was added to a two-neck bottle containing pentafluorobenzoic acid (2 mmol, 424 mg), diphenyl diselenide (3mmol, 936 mg), $Cu(OAc)_2$(1.5 mmol，300 mg), 1,10-Phenanthroline (1.5 mmol，270 mg), K_2CO_3 (6 mmol, 828 mg) under oxygen. The reaction mixture was stirred at 150 °C for 22 h. After cooling down, the reaction mixture was diluted with 10 mL of ethyl ether and filtered through a pad of silica gel. The solvent was removed under vacuum. The crude product was purified by silica gel column chromatography (petroleum ether) to afford the product as a white

solid (497 mg, 54%). ^{1}H NMR (500 MHz, DMSO) δ 7.53 – 7.46 (m, 4H), 7.35 – 7.31 (m, 6H). ^{19}F NMR (376 MHz, DMSO) δ -126.70 (s, 1H). ^{13}C NMR (101 MHz, DMSO) δ 132.29, 130.25, 129.04, 128.55. GC-MS (m/z) calcd for $C_{18}H_{10}F_4Se_2$ $[M]^+$: 462; Found: 462.

9,9',9'',9'''-(3,6-bis(phenylselanyl)benzene-1,2,4,5-tetrayl) tetrakis(9H-carbazole) (CzSe)

60% NaH (144 mmol, 5.76 g) was added to carbazole (18 mmol, 3.00 g) in 100 mLDMF. After reacting at room temperature for 30 minutes, a DMF (100 mL) solution of 2Se4F (3 mmol, 1.38 g) was added to the system and reacted for 15 h at 80°C. After cooling to room temperature, deionized water was added and stirred for 30 minutes. The mixture was filtered and the filter cake was collected. The crude product was purified by silica gel column chromatography (petroleum ether /dichloromethane=1/2, v/v) to afford the product, followed by recrystallization from THF to afford CzSe (1.8 g, 60%) as a pale-yellow solid. ^{1}H NMR (500 MHz, $CDCl_3$) δ 7.61 (d, *J* = 7.5 Hz, 8H), 7.13 (d, *J* = 8.1 Hz, 8H), 7.10 – 7.04 (m, 8H), 6.99 (dd, *J* = 10.8, 3.9 Hz, 8H), 6.38 (t, *J* = 7.1 Hz, 2H), 6.30 – 6.17 (m, 8H). ^{13}C NMR (101 MHz, DMSO, 110^{o}C) δ 139.96, 132.90, 128.31, 127.50, 124.98, 123.27, 120.06, 119.73, 111.99. MALDI TOF-MS: calcd for $C_{66}H_{42}N_4Se_2$[M]$^+$: 1050.2; found: 1050.2.

2.Photophysical measurements

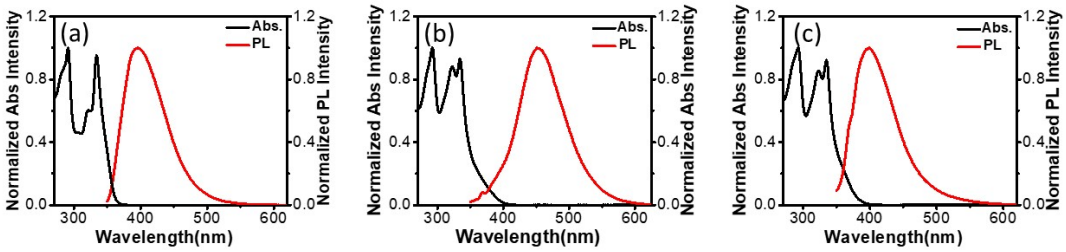

Fig. S1 UV-vis and PL spectra of (a) CzO, (b) CzS and (c) CzSe and in THF solution at room temperature (λ_{ex} = 330 nm, 10 μM).

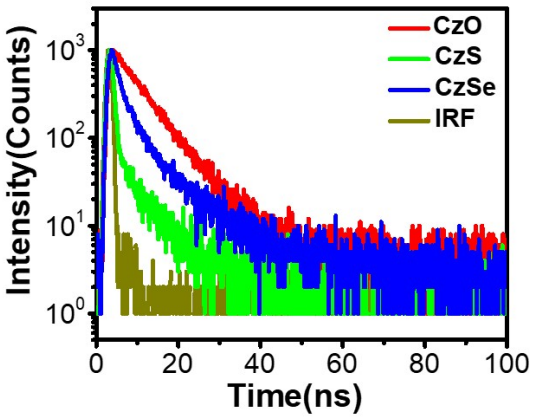

Fig. S2 Lifetime decay curves of CzO, CzS, CzSe and instrument response function (IRF) in THF solution at room temperature (10 μM).

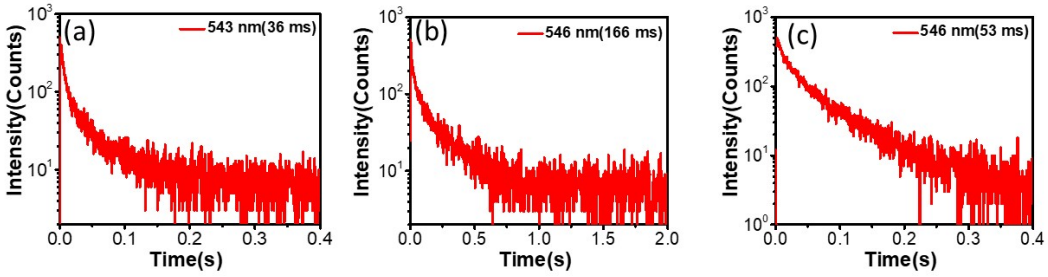

Fig. S3 Lifetime decay curves of (a)CzO, (b) CzS and (c) CzSe in neat films at room temperature under air.

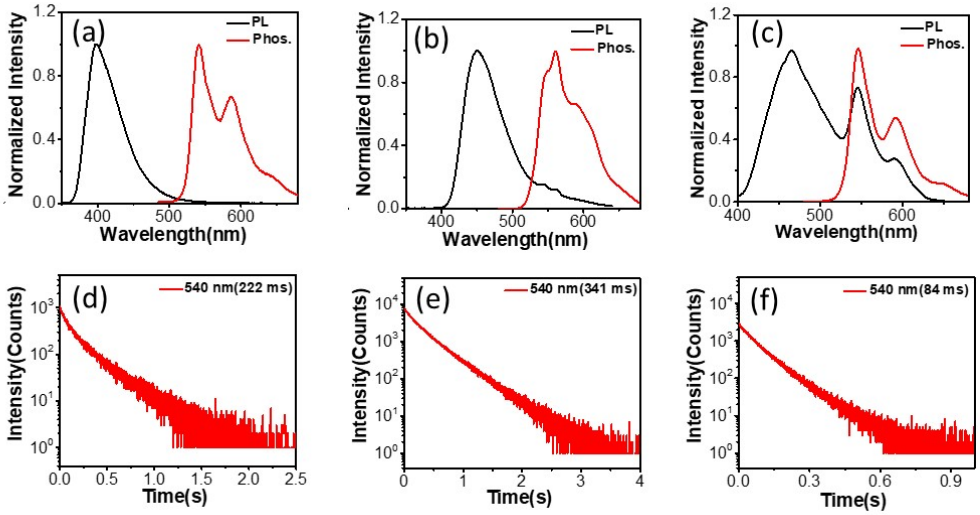

Fig. S4 Steady-state spectra and delay spectra (delay time: 10 ms) of (a) CzO, (b) CzS and (c) CzSe in crystal at room temperature under air. Lifetime decay curves of (d)CzO, (e) CzS and (f) CzSe in crystal at room temperature under air.

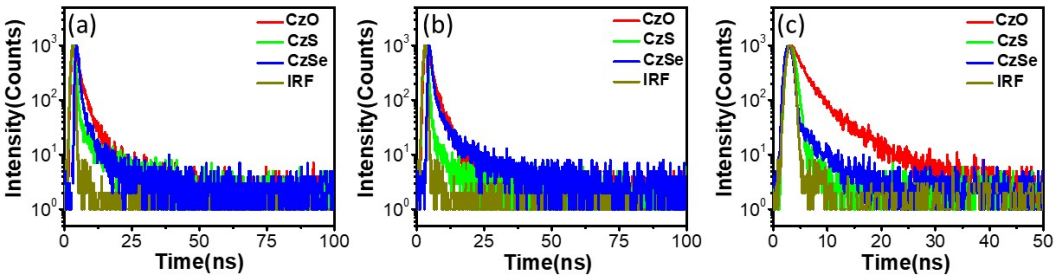

Fig. S5 Fluorescence lifetime of CzO, CzS, CzSe and IRF (a)in PVA films, (b) in neat films and (c) in crystal at room temperature.

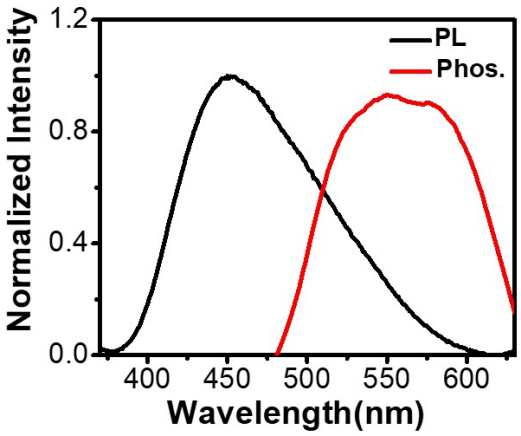

Fig. S6 Steady-state spectra and delay spectra (delay time: 10 ms) of 6wt% CzS doped in DOPEO at room temperature.

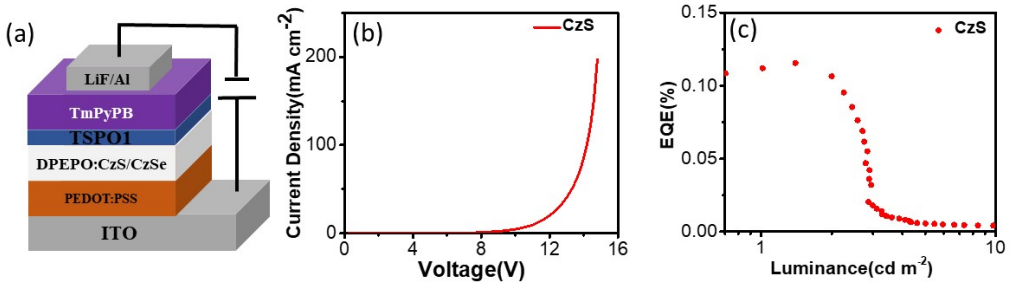

Fig. S7 (a) Device configuration, (b) current-density (J)–voltage (V) characteristics (c) EQE-luminance characteristics of the solution-processed OLEDs based on CzS with white emission.

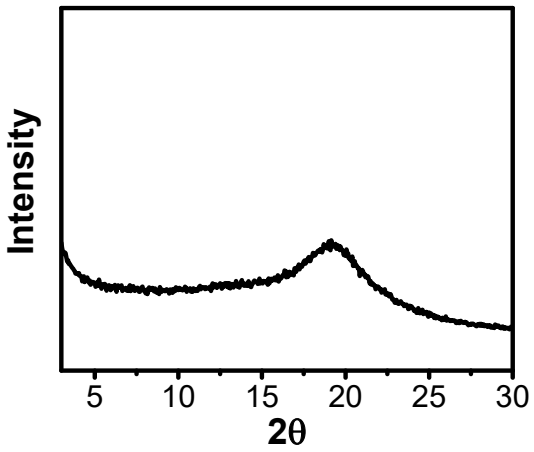

Fig. S8 XRD patterns of CzS in PVA film.

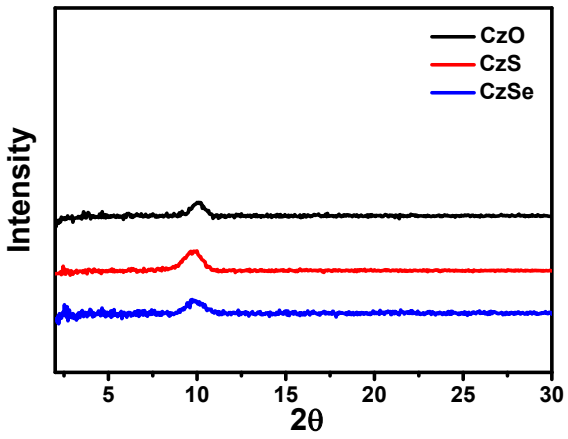

Fig. S9 XRD patterns of CzO, CzS and CzSe in neat film.

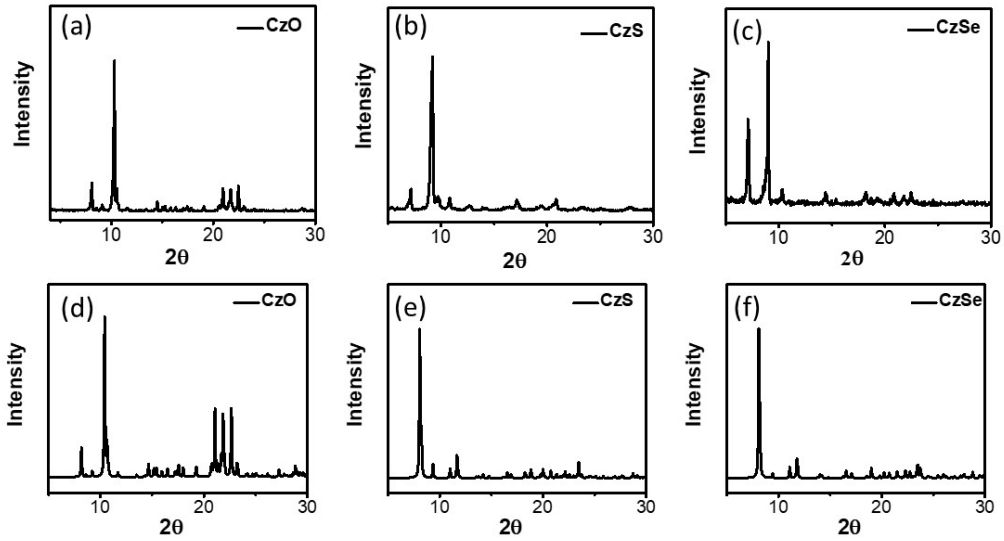

Fig. S10 Experimental XRD patterns of (a)CzO, (b)CzS, (c)CzSe in crystal state. Predicted XRD patterns of (d)CzO, (e)CzS, (f)CzSe in crystal state.

The XRD of crystal powder of three molecules show sharp peaks, which were similar to the predicted XRD patterns from single crystals. In neat film, the diffraction signals are consistent with those in the crystal, but become very weak, revealing the receded crystallinity and less ordered molecular packing. In PVA film, only diffraction peaks of PVA can be observed for all the molecules.

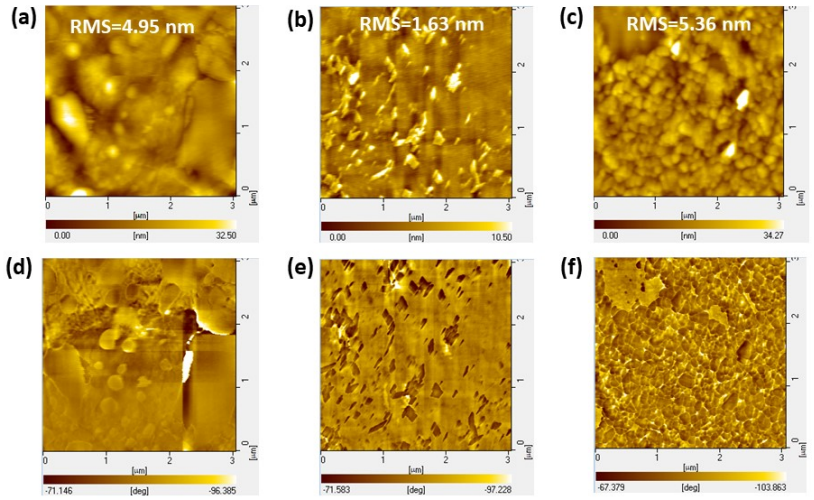

Fig. S11 AFM height and phase images of CzO (a, d), CzS (b, e) and CzSe (c, f) in neat films.

The neat films were obtained by drop-coating the solution (about 2 mg/ml in THF) of three materials on the glass substrates. As seen in the AFM images, the average root-

mean-square (RMS) roughness of the films based on CzO, CzS and CzSe are 4.95 nm, 1.63 nm and 5.36 nm, respectively.

The intersystem crossing (ISC) rate constant (k_{ISC}), the ISC efficiency (Φ_{ISC}), the radiative rate constant of phosphorescence (k_r^P) of CzO, CzS and CzSe were calculated according to the following equations:

$$\Phi_{FL} = 1 - \Phi_{ISC} - \Phi_{nr}^{F} \quad \text{(S1)}$$

$$\Phi_{Ph} = \Phi_{ISC} - \Phi_{nr}^{P} - \Phi_{q} \quad \text{(S2)}$$

$$k_r^F = \frac{\Phi_{FL}}{\tau_{FL}} \quad \text{(S3)}$$

$$k_{ISC} = \frac{\Phi_{ISC}}{\tau_{FL}} \quad \text{(S4)}$$

$$\frac{1}{\tau_{FL}} = k_r^F + k_{nr}^F + k_{ISC} \quad \text{(S5)}$$

$$\Phi_{FL} = \frac{k_r^F}{k_r^F + k_{nr}^F + k_{ISC}} \quad \text{(S6)}$$

$$\frac{1}{\tau_{Ph}} = k_r^P + k_{nr}^P + k_q \quad \text{(S7)}$$

$$\Phi_{Ph} = \frac{\Phi_{ISC} k_r^P}{k_r^P + k_{nr}^P + k_q} \quad \text{(S8)}$$

where Φ_{FL} and Φ_{Ph} are the absolute quantum yield of fluorescence and phosphorescence, and Φ_{nr}^{F} and Φ_{nr}^{P} is the nonradiative yield of fluorescence and phosphorescence, and $\tau_{FL}$and τ_{Ph} are the average lifetime of fluorescence and

phosphorescence, and k_{nr}^{F} is the nonradiative constant of fluorescence, and k_q ia the quenching rate of T_1 phosphorescence.[6,7]

Table S1. Summary of rate constants of of CzO, CzS and CzSe doped in PVA film in vacuo.

	Φ_{ISC} [%]	k_{ISC} [s^{-1}]	k_r^p [s^{-1}]	$k_{nr}+k_q$ [s^{-1}]
CzO	69.0	$2.5x10^8$	$2.7x10^{-2}$	1.2
CzS	96.8	$3.6\ x10^8$	0.12	2.0
CzSe	99.5	$4.8\ x10^8$	0.11	6.9

Table S2. Summary of rate constants of of CzO, CzS and CzSe in neat film under ambient conditions.

	Φ_{ISC} [%]	k_{ISC} [s^{-1}]	k_r^p [s^{-1}]	$k_{nr}+k_q$ [s^{-1}]
CzO	74.2	$2.9\ x10^8$	0.69	27.1
CzS	96.2	$6.9\ x10^8$	0.33	5.7
CzSe	99.7	$3.0\ x10^8$	0.17	18.7

Table S3. Summary of rate constants of of CzO, CzS and CzSe in crystal states under ambient conditions.

	Φ_{ISC} [%]	k_{ISC} [s^{-1}]	k_r^p [s^{-1}]	$k_{nr}+k_q$ [s^{-1}]
CzO	75.9	$2.1\ x10^8$	$4.5x10^{-2}$	4.5
CzS	96.8	$14.2\ x10^8$	$7.6\ x10^{-2}$	2.9
CzSe	99.9	$7.6\ x10^8$	$4.8\ x10^{-2}$	11.9

3. X-ray crystallographic analysis

The single crystal of CzO was cultivated by the solvent diffusion method in THF and methanol. The single crystals of CzS and CzSe were cultivated by the solvent diffusion method in THF and n-hexane. The single crystal X-ray diffraction experiments were carried out using a Bruker Smart APEX diffractometer with CCD area detector and graphite monochromator, Mo Kα radiation (λ =0.71073 Å). The intensity data were recorded with ω scan mode. Lorentz, polarization factors were made for the intensity data and absorption corrections were performed using SADABS program. The crystal structure was determined using the SHELXTL program and refined using full matrix least squares. All non-hydrogen atoms were assigned with anisotropic displacement parameters, whereas hydrogen atoms were placed at calculated positions theoretically and included in the final cycles of refinement in a riding model along with the attached carbons. Thus, obtained crystallographic parameters of CzO, CzS and CzSe were summarized in Table S4 and CCDC reference number is 2071757, 2071758 and 2071759.

Table S4. Single crystal data of CzO, CzS and CzSe.

Compound	**CzO**	**CzS**	**CzSe**
Empirical formula	$C_{66}H_{42}N_4O_2$	$C_{66}H_{42}N_4S_2$	$C_{66}H_{42}N_4Se_2$
Formula weight	922.33	954.29	1050.17
Temperature	173.0 K	298.0 K	180.0 K
Crystal system	Monoclinic	Monoclinic	Monoclinic
Space group	C2/c	$P2_1/n$	$P2_1/n$
Unit cell dimensions	a=20.9207(9) Å	a=12.484(6) Å	a = 12.4514(6) Å
	b=13.0711(5) Å	b=10.476(4) Å	b = 10.3555(5) Å
	c=18.5269(13) Å	c=21.89(1) Å	c = 21.7942(11) Å
	alpha=90°	alpha=90°	alpha = 90°
	beta=113.710(1)°	beta=91.476(14)°	beta = 90.658(2) °
	gamma=90°	gamma=90°	gamma = 90°
Volume	4638.7(4) $Å^3$	2862(2) $Å^3$	2810.0(2) $Å^3$
Z	4	4	4
Density	1.322	1.108	1.240
F (000)	1928.0	996.0	1068.0
2θ range for data collection	4.252 to 70.178°	5.076 to 52.102°	4.354 to 49.426°
Index ranges	$-33 \le h \le 27$, $-21 \le k \le 19$, $-25 \le l \le 29$	$-15 \le h \le 15$, $-12 \le k \le 12$, $-26 \le l \le 26$	$-14 \le h \le 13$, $-12 \le k \le 12$, $-25 \le l \le 25$
Reflections collected	53438	42986	34291
Independent reflections	9317 [R_{int} = 0.0960]	5599 [R_{int} = 0.1021]	4788 [R_{int} = 0.0497]
Data/restraints/parameters	9317/102/325	5599/0/326	4788/0/325
Goodness-of-fit on F^2	1.017	1.087	1.104
Final R indexes [I>=2σ (I)]	R_1 = 0.0834, wR_2 = 0.1518	R_1 = 0.0727, wR_2 = 0.2185	R_1 = 0.0449, wR_2 = 0.1313
Final R indexes [all data]	R_1 = 0.2266, wR_2 = 0.1984	R_1 = 0.0998, wR_2 = 0.2406	R_1 = 0.0570, wR_2 = 0.1374
Largest diff. peak and hole	0.30 and -0.23 e $Å^{-3}$	0.34 and -0.26 e $Å^{-3}$	0.40 and -0.32 e $Å^{-3}$
CCDC	2071757	2071758	2071759

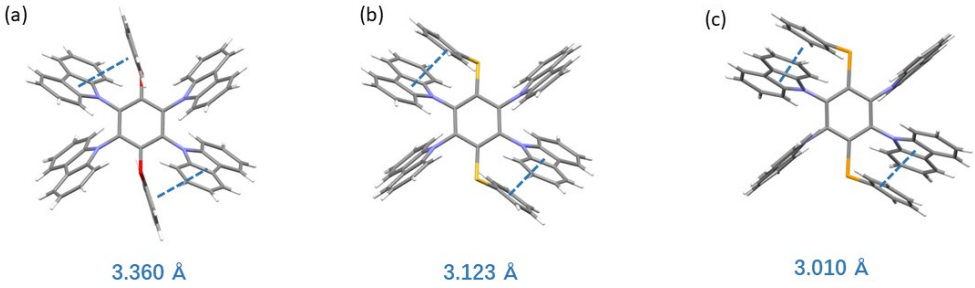

Fig. S12 Distances between the benzene ring and the centroid of the carbazole unit.

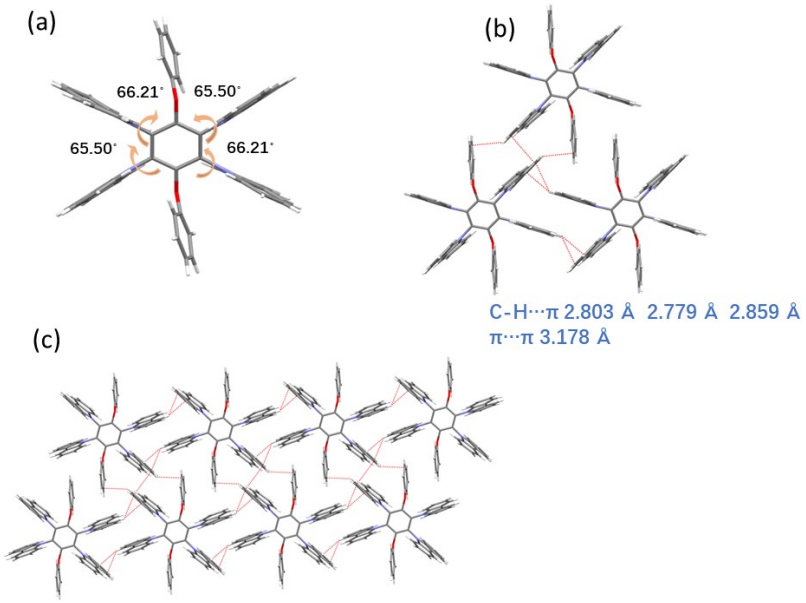

Fig. S13 Single crystal structure of CzO and associated intermolecular interactions.

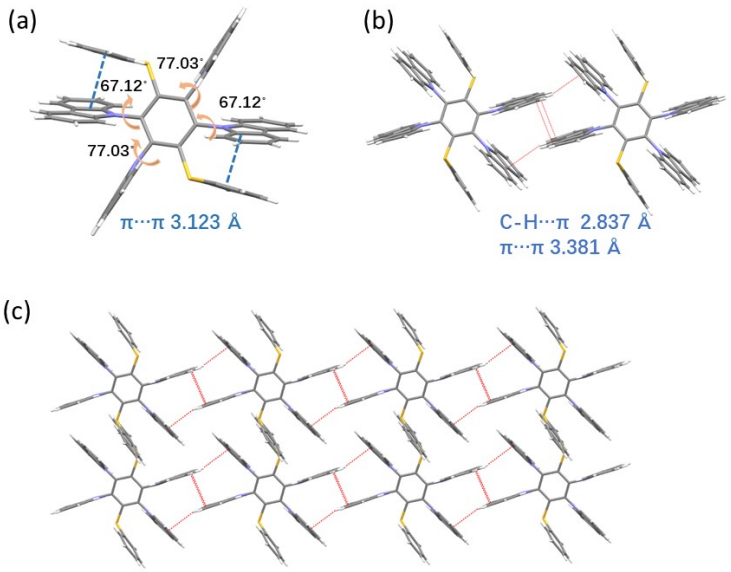

Fig. S14 Single crystal structure of CzS and associated intermolecular interactions.

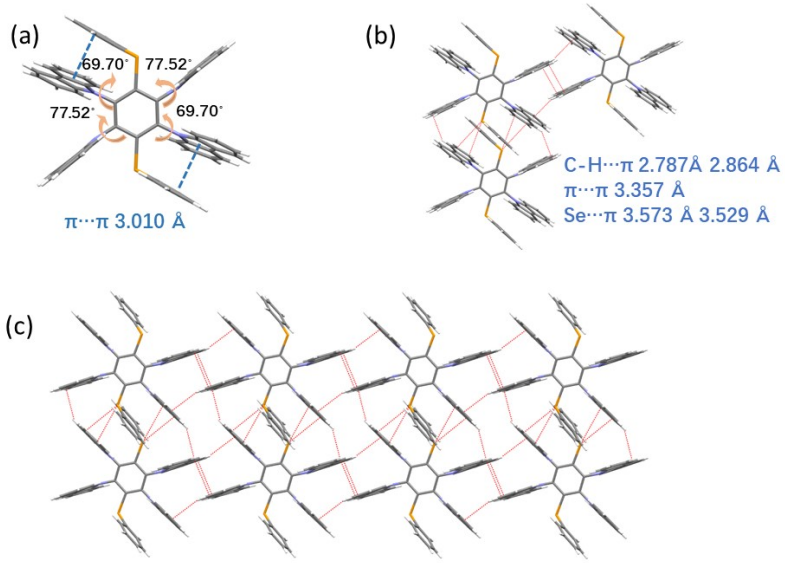

Fig. S15 Single crystal structure of CzSe and associated intermolecular interactions.

4. Theoretical calculation results

Density functional theory (DFT) and time-dependent DFT (TD-DFT) calculations were carried out at the M06-2x/def2-SV level using on Gaussian 09 package.[8] CzO, CzS and CzSe were directly optimized to obtain the S_0 geometry. The orbital coupling constant (SOC) were carried out at the M06-2x/def2-SV level using on ORCA 4.1.0.[9] The SOC is calculated using optimized S_0 geometry. The TDDFT calculations for all molecules are performed using the optimized S_0 geometry. The hole and electron distribution analysis of T_1 is performed by Multiwfn program.[10]

Table S5. The singlet and triplet excited state transition configurations of CzO. $T_n <$ S_1 were marked in light green.

Excited state	Energy (eV)	Energy gap (S_1-T_n)	SOC (S_1-T_n)
S_1	3.9972		
T_1	3.3967	0.6005	0.5500
T_2	3.6120	0.3852	0.1900
T_3	3.6215	0.3757	0.2973
T_4	3.6600	0.3372	0
T_5	3.6652	0.3320	0.1456
T_6	3.7465	0.2507	0.7273
T_7	3.8296	0.1676	0.0849
T_8	3.8330	0.1642	0.0900
T_9	3.8467	0.1505	0.0316
T_{10}	3.8585	0.1387	0.1500
T_{11}	4.0035	-0.0063	0.0700

Table S6. The singlet and triplet excited state transition configurations of CzS. $T_n < S_1$ were marked in light green.

Excited state	Energy (eV)	Energy gap (S_1-T_n)	SOC (S_1-T_n)
S_1	3.9597		
T_1	3.2975	0.6622	0.0849
T_2	3.5954	0.3643	0.0000
T_3	3.6314	0.3283	0.0990
T_4	3.6352	0.3245	0.2456
T_5	3.6512	0.3085	0.2402
T_6	3.6799	0.2798	1.5698
T_7	3.7169	0.2428	2.2912
T_8	3.8110	0.1487	0.2733
T_9	3.8181	0.1416	0.1980
T_{10}	3.8216	0.1381	0.7365
T_{11}	3.8317	0.1280	0.1697
T_{12}	3.9106	0.0491	1.7071
T_{13}	4.0373	-0.0776	0.4101

Table S7. The singlet and triplet excited state transition configurations of CzSe. $T_n < S_1$ were marked in light green.

Excited state	Energy (eV)	Energy gap (S_1-T_n)	SOC (S_1-T_n)
S_1	3.9792		
T_1	3.3237	0.6555	2.3200
T_2	3.5949	0.3843	0.7300
T_3	3.6222	0.3570	0.1900
T_4	3.6348	0.3444	0.4079
T_5	3.6399	0.3393	0.8603
T_6	3.6885	0.2907	6.7300
T_7	3.7021	0.2771	16.6461
T_8	3.8031	0.1761	4.0250
T_9	3.8045	0.1747	1.7159
T_{10}	3.8053	0.1739	0.7800
T_{11}	3.8217	0.1575	1.2600
T_{12}	3.9524	0.0268	11.1236
T_{13}	4.0167	-0.0375	5.1200

Table S8. The reorganization energy of the T_1 to S_0 ($\lambda_{T1\text{-}S0}$) transition.[11]

	CzO	CzS	CzSe
$\lambda_{T1\text{-}S0}$ (eV)	0.89	0.63	0.62

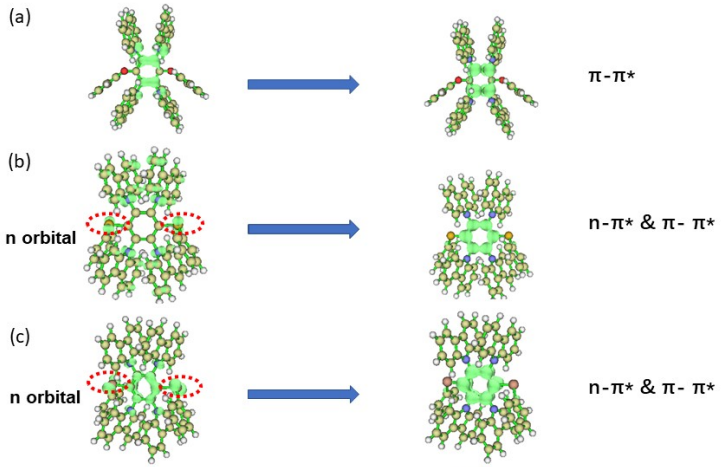

Fig. S16 Hole-electron distributions of T_1 states of (a)CzO, (b)CzS and (c)CzSe.

5.Reference

1. L.-C. Campeau, M. Parisien, A. Jean and K. Fagnou, *J. Am. Chem. Soc.*, 2006, **128**, 581-590.
2. Z. Liu, K. Ouyang and N. Yang, *Org. Biomol. Chem.*, 2018, **16**, 988-992.
3. J. Wang, H. Li, T. Leng, M. Liu, J. Ding, X. Huang, H. Wu, W. Gao and G. Wu, *Org. Biomol. Chem.*, 2017, **15**, 9718-9726.
4. I. Bhattacharjee and S. Hirata, *Adv. Mater.,* 2020, **32**, 2001348.
5. S. Wang, H. Shu, X. Han, X. Wu, H. Tong and L. Wang, *J. Mater. Chem. C*, 2021, **9**, 9907-9913.
6. R. Huang, J. S. Ward, N. A. Kukhta, J. Avo, J. Gibson, T. Penfold, J. C. Lima, A. S. Batsanov, M. N. Berberan-Santos, M. R. Bryce and F. B. Dias, *J. Mater. Chem. C*, 2018, **6**, 9238-9247.
7. Y. Li, L. Jiang, W. Liu, S. Xu, T. Y. Li, F. Fries, O. Zeika, Y. Zou, C. Ramanan, S. Lenk, R. Scholz, D. Andrienko, X. Feng, K. Leo and S. Reineke, *Adv. Mater.*, 2021, **33**, 2101844.
8. M. J. Frisch, G. W. Trucks, H. B. Schlegel, G. E. Scuseria, M. A. Robb, J. R. Cheeseman, G. Scalmani, V. Barone, B. Mennucci, G. A. Petersson, H. Nakatsuji, M. Caricato, X. Li, H. P. Hratchian, A. F. Izmaylov, J. Bloino, G. Zheng, J. L. Sonnenberg, M. Hada, M. Ehara, K. Toyota, R. Fukuda, J. Hasegawa, M. Ishida, T. Nakajima, Y. Honda, O. Kitao, H. Nakai, T. Vreven, J. A. Montgomery, Jr., J. E. Peralta, F. Ogliaro, M. Bearpark, J. J. Heyd, E. Brothers, K. N. Kudin, V. N. Staroverov, T. Keith, R. Kobayashi, J. Normand, K. Raghavachari, A. Rendell, J. C. Burant, S. S. Iyengar, J. Tomasi, M. Cossi, N. Rega, J. M. Millam, M. Klene, J. E. Knox, J. B. Cross, V. Bakken, C. Adamo, J. Jaramillo, R. Gomperts, R. E. Stratmann, O. Yazyev, A. J. Austin, R. Cammi, C. Pomelli, J. W. Ochterski, R. L. Martin, K. Morokuma, V. G. Zakrzewski, G. A. Voth, P. Salvador, J. J. Dannenberg, S. Dapprich, A. D. Daniels, O. Farkas, J. B. Foresman, J. V. Ortiz, J. Cioslowski, and D. J. Fox, Gaussian 09, Revision D.01, Gaussian, Inc., Wallingford CT, 2013.
9. U. Ekstrom, L. Visscher, R. Bast, A. J. Thorvaldsen and K. Ruud, *J. Chem. Theory Comput.*, 2010, **6**, 1971-1980.
10. T. Lu and F. Chen, *J. Comput. Chem*., 2012, **33**, 580-592.
11. H. Zhu, I. Badía-Domínguez, B.Shi, Q. Li, P. Wei, H. Xing, M. C. R. Delgado and F. Huang, *J. Am. Chem. Soc.*, 2021, **143**, 2164-2169.